Title

Canonical/β-Catenin Wnt Pathway Activation Improves Retinal Pigmented Epithelium Derivation From Human Embryonic Stem CellsCanonical Wnt Signaling in RPE Differentiation

Journal

Investigative Ophthalmology & Visual Science, 56(2)

ISSN

0146-0404

Authors

Leach, Lyndsay L
Buchholz, David E
Nadar, Vignesh P
et al.

Publication Date

2015-02-11

DOI

10.1167/iovs.14-15835

Peer reviewed

Canonical/β-Catenin Wnt Pathway Activation Improves Retinal Pigmented Epithelium Derivation From Human Embryonic Stem Cells

Lyndsay L. Leach,[1–3] David E. Buchholz,[1–3] Vignesh P. Nadar,[1,4] Stefan E. Lowenstein,[3] and Dennis O. Clegg[1–3]

[1]Center for Stem Cell Biology and Engineering, University of California, Santa Barbara, California, United States
[2]Neuroscience Research Institute, University of California, Santa Barbara, California, United States
[3]Department of Molecular, Cellular & Developmental Biology, University of California, Santa Barbara, California, United States
[4]California State University, Channel Islands, California, United States

Correspondence: Dennis O. Clegg, Neuroscience Research Institute, University of California, Santa Barbara, CA 93106, USA; clegg@lifesci.ucsb.edu.

Submitted: October 8, 2014
Accepted: January 5, 2015

Citation: Leach LL, Buchholz DE, Nadar VP, Lowenstein SE, Clegg DO. Canonical/β-catenin Wnt pathway activation improves retinal pigmented epithelium derivation from human embryonic stem cells. *Invest Ophthalmol Vis Sci*. 2015;56:1002–1013. DOI:10.1167/iovs.14-15835

Purpose. The purpose of this study was to better understand the role canonical/β-catenin Wnt signaling plays in the differentiation of human embryonic stem cells (hESCs) into retinal pigmented epithelium (RPE), with the goal of improving methods for derivation.

Methods. Fluorescent reporters were generated to monitor RPE differentiating from hESCs by using a previously described 14-day derivation protocol. Reporters were used to test the effects of the canonical/β-catenin Wnt pathway agonist CHIR99021 on differentiating RPE. Cells derived from differentiation studies were characterized by lineage-specific transcription factor expression, morphology, pigmentation, and function. The RPE derivation efficiency was determined from percentage positive PMEL17 expression.

Results. Fluorescent reporters mimicked expression of endogenous genes during 14-day differentiation to RPE. Analysis of Wnt pathway gene expression showed that the pathway components are expressed in differentiating RPE cells. Addition of CHIR99021 improved RPE derivation based on morphology, expression of RPE-specific lineage markers, and genes involved in melanogenesis. Additionally, expression of the neural retina marker CHX10 was suppressed during differentiation with CHIR99021. Addition of soluble WNT3A, but not WNT5A, had the same result. The CHIR99021-modified protocol yielded cell populations that were 97.77% ± 0.1% positive for the RPE marker PMEL17 at day 14. After cells were expanded to passage 3, they were shown to express RPE markers, carry out phagocytosis of rod outer segments, and secrete pigment epithelium–derived factor apically and vascular endothelial growth factor basally.

Conclusions. Our findings demonstrated the importance of canonical/β-catenin Wnt signaling in RPE differentiation and showed that manipulating the pathway significantly improves RPE derivation from hESC.

Keywords: retinal pigmented epithelium, human embryonic stem cells, age-related macular degeneration, Wnt signaling, fluorescent reporters

Sight is perhaps the most critical of our sensory modalities. The ability to see allows us to navigate our surroundings and perform almost all of our everyday tasks with ease. Diseases causing blindness not only present a large health care burden, but also deplete quality of life. Age-related macular degeneration (AMD) is one such disease, recognized as a leading cause for blindness in the elderly in the developed world.[1–3] Age-related macular degeneration is characterized by dysfunction and death of the highly specialized retinal pigmented epithelium (RPE), which supports and maintains the health and function of the photoreceptors. Progressive loss of healthy RPE in the macula results in impairment of central visual acuity. At present, there are no treatment options for the more common "dry," or atrophic, form of AMD, which comprises 80% to 90% of patient cases.[4] Typified by regions of "geographic atrophy," where RPE and photoreceptor cells have been lost, this form of AMD is a candidate disease for cell-based therapies to replace diseased RPE with RPE derived from pluripotent cells.

The RPE can be derived from stem cells in vitro by several methods. The continuous adherent culture method[5–8] is currently used to derive RPE of clinical quality; however, this takes 6 to 7 months to produce cells, representing a bottleneck for clinical translation. Our group and others have used a more directed approach to deriving RPE by using exogenous cues essential for RPE development in vivo.[9–12] Our protocol pushes human embryonic stem cells (hESCs) to rapidly differentiate to an RPE lineage in 14 days with nearly 80% efficiency.[9] However, this and other methods do not achieve complete conversion and require mechanical enrichment of cells after differentiation. The goal of this study was to improve RPE derivation by better understanding how RPE cells differentiate from hESCs, a process that remains poorly defined.

Recent reports identify the requirement for Wnt signaling in RPE development in vivo.[13,14] In mice, elements of the canonical/β-catenin Wnt signaling pathway are expressed in the presumptive RPE,[15,16] and β-catenin regulates two key RPE differentiation factors: orthodenticle homeobox 2 protein (Otx2) and microphthalmia-associated transcription factor (Mitf).[13,17] Furthermore, canonical/β-catenin Wnt signaling and Otx2 together can specify RPE during chick eye development.[18] Although Wnt signaling is important for RPE development in vivo, many protocols deriving RPE from pluripotent stem cells include treatments to inhibit Wnt signaling.[9,12,19] Recently, it was shown that activating canonical/β-catenin Wnt signaling by using the glycogen synthase kinase-3 β (GSK3β) inhibitor CHIR99021 in 3D hESC-derived optic cup cultures promotes MITF expression and pigmentation.[20] Wnt pathways are context and species dependent[21] and the impact of Wnt signaling on different stages of RPE differentiation from hESCs is not well understood.

The 14-day protocol provides a unique and time-efficient framework for modeling human ocular development in vitro as cells progress from early neural/eye field lineages to RPE.[9] In this study, we developed fluorescent reporter hESC lines to investigate Wnt signaling. We showed that elements of the Wnt signaling pathway are upregulated during directed differentiation to RPE, using the 14-day method, and that CHIR99021 improves efficiency of RPE derivation from hESCs.

Methods

Cell Culture

Human embryonic stem cells (UCSF4, NIH registry No. 0044; University of California, San Francisco, CA, USA) were maintained in 6-well plates in mTeSR1 medium (StemCell Technologies, Vancouver, BC, Canada) and passaged every 5 to 7 days. H9-derived (WiCell Research Institute, Madison, WI, USA) and UCSF4-derived hESC-RPE cells were maintained in X-VIVO 10 medium (Lonza, Walkersville, MD, USA).[22] Human fetal RPE (hfRPE) cells (provided by L. Johnson, Center for the Study of Macular Degeneration, University of California, Santa Barbara, CA, USA; and D. Bok, Jules Stein Eye Institute, University of California, Los Angeles, CA, USA) were maintained in media formulated by Maminishkis et al.[23] UCSF4, hESC-RPE, and hfRPE cells were cultured on Matrigel (BD Biosciences, San Diego, CA, USA). Human umbilical vein endothelial cells (HUVECs; PromoCell, Heidelberg, Germany) were maintained on 0.1% gelatin in Endothelial Cell Growth Medium (PromoCell).

Fluorescent Reporter Vectors and Lentivirus Particle Preparation

Human RAX (−1092 bp to −92 bp relative to ATG), OTX2 (−5996 bp to −4965 bp relative to ATG of OTX2 isoform A),[24] MITF-D (−3046 bp to −2847 bp relative to ATG),[25] and RPE65 (−1069 bp to −16 bp relative to ATG)[26] promoter sequences were cloned into the HIV (human immunodeficiency virus)–based self-inactivating (SIN) aMHC-mCherry-Rex-Blasticidin lentiviral vector[27] (plasmid No. 21228; Addgene, Cambridge, MA, USA) by using *Not*I and *Age*I restriction sites. The vector contains the blasticidin resistance gene, under control of the REX1 promoter, providing selection only in pluripotent cells, not in differentiating cultures or mature RPE.

Lentivirus particles were prepared as described previously,[28] with modification. The calcium phosphate method was used to transiently transfect 5.4×10^6 human embryonic kidney (HEK) 293T cells (per T150 flask) with 54 μg transfer vector, 16.2 μg vesicular stomatitis virus G (VSV-G) protein envelope vector (pMD2.G; Addgene), and 40.5 μg packaging vector (psPAX2; Addgene). Lentivirus particles were precipitated at 4°C by using PEG-it Virus Precipitation Solution (System Biosciences, Mountain View, CA, USA) and isolated according to the manual. Viral titer was determined by using lysates from HT1080 cells (ATCC, Manassas, VA, USA) transduced by using Transdux (System Biosciences), according to the protocol. Cell lysates were processed and analyzed by using the Global Ultra Rapid Titer Kit (System Biosciences). All cell lines were transduced for 24 hours with concentrated virus stock, added directly to fresh growth medium containing 8 μg/mL polybrene.

Generating Stable Fluorescent Reporter hESC Lines

UCSF4 cells were passaged to 12-well plates for transduction. Growth media containing 10 μM Y-27632 (Tocris Bioscience, Bristol, UK) was added 1 hour before passaging. Approximately 10 hESC colonies (averaging ~10,000 cells/colony) per 12-well to be plated were manually dissected into small clumps. Clumps were pelleted for 5 minutes at 94*g* and resuspended in growth media with 10 μM Y-27632 and 8 μg/mL polybrene. The hESCs were transduced at a multiplicity of infection (MOI) of 30 (30 virus particles per one cell). Viral particles, polybrene, and Y-27632 were washed out 24 hours post transduction and media was replenished every day for 4 days. Cultures were then treated with 5 μg/mL blasticidin to select for cells with transgene integration. Stably transduced colonies were expanded and maintained in mTeSR1 media containing 5 μg/mL blasticidin until differentiated. Differentiating cells were imaged on an Olympus IX71 inverted tissue culture microscope (Olympus, Center Valley, PA, USA) in the TRITC channel with ~250-ms exposure time.

Human Embryonic Stem Cell Differentiation to RPE

The UCSF4 colonies were passaged by using EDTA[29] (Life Technologies, Carlsbad, CA, USA) and differentiated to RPE by using the protocol developed by Buchholz et al.[9] The protocol was modified to include 3 μM CHIR99021 (Stemgent, Cambridge, MA, USA) from day 8 to 14. For experiments using Wnt ligands, human WNT3A or WNT5A recombinant protein (100 ng/mL[30]; R&D Systems, Inc., Minneapolis, MN, USA) was added to differentiation media from day 8 to 14. On day 14, RPE cells were manually enriched to passage 0 as previously described[9] and maintained in X-VIVO 10 supplemented with 10 μM Y-27632 for 4 to 7 days. Passage 0 UCSF4-RPE cells were expanded to passage 2 (passaging every 30 days) and cryopreserved, generating an intermediate cell bank (ICB).[22,31] The ICB cells were thawed to passage 3 for functional tests.

Quantitative Real-Time Polymerase Chain Reaction (qRT-PCR)

Total RNA was purified by using the RNeasy Plus Mini Kit (Qiagen, Hilden, Germany). RNA was converted to cDNA by using the iScript cDNA Synthesis Kit (Bio-Rad, Hercules, CA, USA). Primer pairs (Supplementary Table S1) were designed to amplify product lengths ranging from 83 to 234 nucleotides that crossed an exon–exon border. The 20-μL reactions were run in 96-well plates and averaged internal triplicates were normalized to the geometric mean of glyceraldehyde phosphate dehydrogenase (*GAPDH*), glucose phosphate isomerase (*GPI*), and hydroxymethylbilane synthase (*HMBS*) housekeeping genes.

For the Human Wnt Signaling Pathway PCR Array (Qiagen), cDNA was synthesized from 0.5 μg total RNA by using the RT^2 First Strand Kit (Qiagen). Instructions for preparing cDNA, RT^2 SYBR Green Mastermix (Qiagen), and 96-well plates were followed directly from the manual. Data were normalized to five housekeeping genes and analyzed by using the $2^{\Delta\Delta CT}$ method. Genes with a fold change greater than 2 and P value $\leq$ 0.05 were represented in the results. All 96-well PCR plates were run on a MyiQ2 Two-Color Real-Time PCR Detection System (Bio-Rad).

Immunocytochemistry (ICC)

Differentiated cells were fixed on day 14 in 12-well plates. Enriched cells were grown in 8-chambered slides and fixed 30 days post passage/thaw. Cells were fixed and blocked as previously described,[32] then labeled with primary antibody (Supplementary Table S2) in blocking solution overnight at 4°C. The next day, cells were washed with PBS and a species-appropriate Alexa Fluor 488 or 555 secondary antibody (Life Technologies) was added for 1 hour at 4°C. Cells were imaged with an Olympus IX71 microscope (12-well plates) or an Olympus BX51 upright microscope (chambered slides).

Flow Cytometry

Differentiated cells were fixed and permeablized as described previously,[9] on day 14. Samples were labeled with unconjugated PMEL17 primary or mouse isotype control antibodies (Dako, Carpinteria, CA, USA) for 30 minutes at room temperature. Samples were then treated with donkey anti-mouse Alexa Fluor 488 secondary antibody for 30 minutes at room temperature. Melanocytes (MeWo) and foreskin fibroblasts (Hs27) were run alongside experimental samples as controls. All samples were run on an Accuri C6 flow cytometer using CFlow software (BD Biosciences). Data were analyzed with FCS Express 4 Flow Cytometry (De Novo Software, Los Angeles, CA, USA). Positive PMEL17 percentage values were determined by setting background levels to 1% positive expression in isotype control antibody-labeled samples from the same cell line.

Functional Assays

For pigment epithelium–derived factor (PEDF) and vascular endothelial growth factor (VEGF) enzyme-linked immunosorbent assays (ELISAs), cells were grown on 24-well transwell inserts for 4 weeks. On the day of media harvest, 20 μL aliquots of growth media were manually pipetted from the top (apical) and bottom (basal) chambers of each transwell to be assayed. Then, 10 μL of the harvested media was diluted (1:5000) and apical and basal PEDF secretion levels were determined by using a Human PEDF ELISA Kit (BioProductsMD, Middletown, MD, USA). The remaining 10 μL of the harvested media was diluted (1:30) and apical and basal VEGF secretion levels were determined by using a Human VEGF ELISA Kit (Life Technologies). For results assaying only PEDF, 10 μL aliquots were harvested from 4-week-old cells seeded to 12-well plates and processed as described herein. The PEDF and VEGF concentrations were normalized to the volume of media (mL) and growth area (mm^2) of the original tissue culture plate.

For bovine rod outer segment (ROS) phagocytosis assays, fresh bovine eyes were purchased from Sierra Medical (Whittier, CA, USA) and ROSs were prepared as previously described,[33] then labeled by using FluoReporter FITC Protein Labeling Kit (Life Technologies). The hESC-RPE, hfRPE, HUVEC, and ARPE-19 cells were cultured by using the methods and media described by Croze et al.[32] After 4 weeks in culture, phagocytosis assays were performed by using the methods and materials described by Buchholz et al.[9] To quantify ROS internalization, each well was imaged on an Olympus IX70 inverted microscope to obtain fluorescent micrographs. Pixel densitometry for three micrographs per condition were analyzed with ImageJ software (http://imagej.nih.gov/ij/; provided in the public domain by the National Institutes of Health, Bethesda, MD, USA) and averaged. All experiments were normalized to pixel densitometry values of the positive control line, ARPE-19, from the respective 96-well plate.

Results

Fluorescent Reporters Reflect Endogenous Gene Expression

To study the effects of various signaling pathways on RPE specification, we sought to develop a set of fluorescent reporters to observe stages of RPE differentiation from hESCs. To do this, lentivirus constructs were generated, whereby the fluorescent reporter gene mCherry is under the control of early eye field and RPE-specific gene promoters: RAX (pre-RPE), OTX2 (pre-RPE, mature RPE), MITF isoform D (MITF-D) (immature RPE, mature RPE), and RPE65 (mature RPE). To test specificity of the reporters, hfRPE, H9-RPE, and HUVEC cells were transduced with reporter lentivirus particles at an MOI of 10. All four reporters showed mCherry fluorescence exclusively in RPE after 4 weeks in culture (Fig. 1A). Control wells for each cell line lacked any observable fluorescence after treatment with 8 μg/mL polybrene (Fig. 1A).

Reporter fluorescence intensities varied with the gene promoter used, which reflected expression levels of endogenous genes, analyzed by qRT-PCR in transduced cells (Fig. 1B). RAX-mCherry reporter fluorescence was analogous to endogenous *RAX* expression levels, which were the lowest in both RPE lines, and observed expression may represent RPE progenitors (Figs. 1A, 1B). RAX expression was anticipated to be low, as differentiated RPE cells have been shown to be Rax negative but to still retain expression of Otx2 and Mitf.[34,35] OTX2-, MITF-D–, and RPE65-mCherry reporter fluorescence appeared higher in H9-RPE than in hfRPE, and similar trends were seen when endogenous *OTX2*, *MITF-D*, and *RPE65* expression was measured (Figs. 1A, 1B). As with reporter fluorescence, HUVECs did not express any RPE-specific genes (Fig. 1B).

Next, hESC lines stably expressing each reporter construct were generated to follow promoter activity during RPE differentiation. Reporter hESC lines were differentiated to RPE by using the 14-day differentiation protocol.[9] Because expression of endogenous *RAX*, *OTX2*, and *MITF* genes has been characterized,[9] this system allowed us to further test reporter specificity. No reporter fluorescence was observed in any stable hESC lines at day 0 (Fig. 2A). On day 4 to 6, RAX-mCherry and OTX2-mCherry fluorescence became visible, then faded out by day 10 to 14 (Fig. 2A), and endogenous levels of *RAX* and *OTX2* gene expression showed a similar trend (Fig. 2B). On day 6 to 14, MITF-D–mCherry fluorescence became observable (Fig. 2A) at the same time that levels of endogenous *MITF* were also detectable (Fig. 2B), consistent with a role for MITF-D during optic vesicle formation and in mature RPE.[9,36] RPE65 is a marker of mature RPE,[4] and neither RPE65-mCherry reporter fluorescence nor endogenous *RPE65* gene expression was detectable from day 0 to 14 (Figs. 2A, 2B), as cells at this stage are thought to be RPE progenitors/immature RPE[9] (for RPE65 reporter expression in mature RPE, see Fig. 5C). These data showed that fluorescent reporters mirror the activity of endogenous promoters.

To determine whether viral integration affected RPE differentiation, enriched passage 0 cultures were examined at 4 weeks. Retinal pigmented epithelium derived from all stable

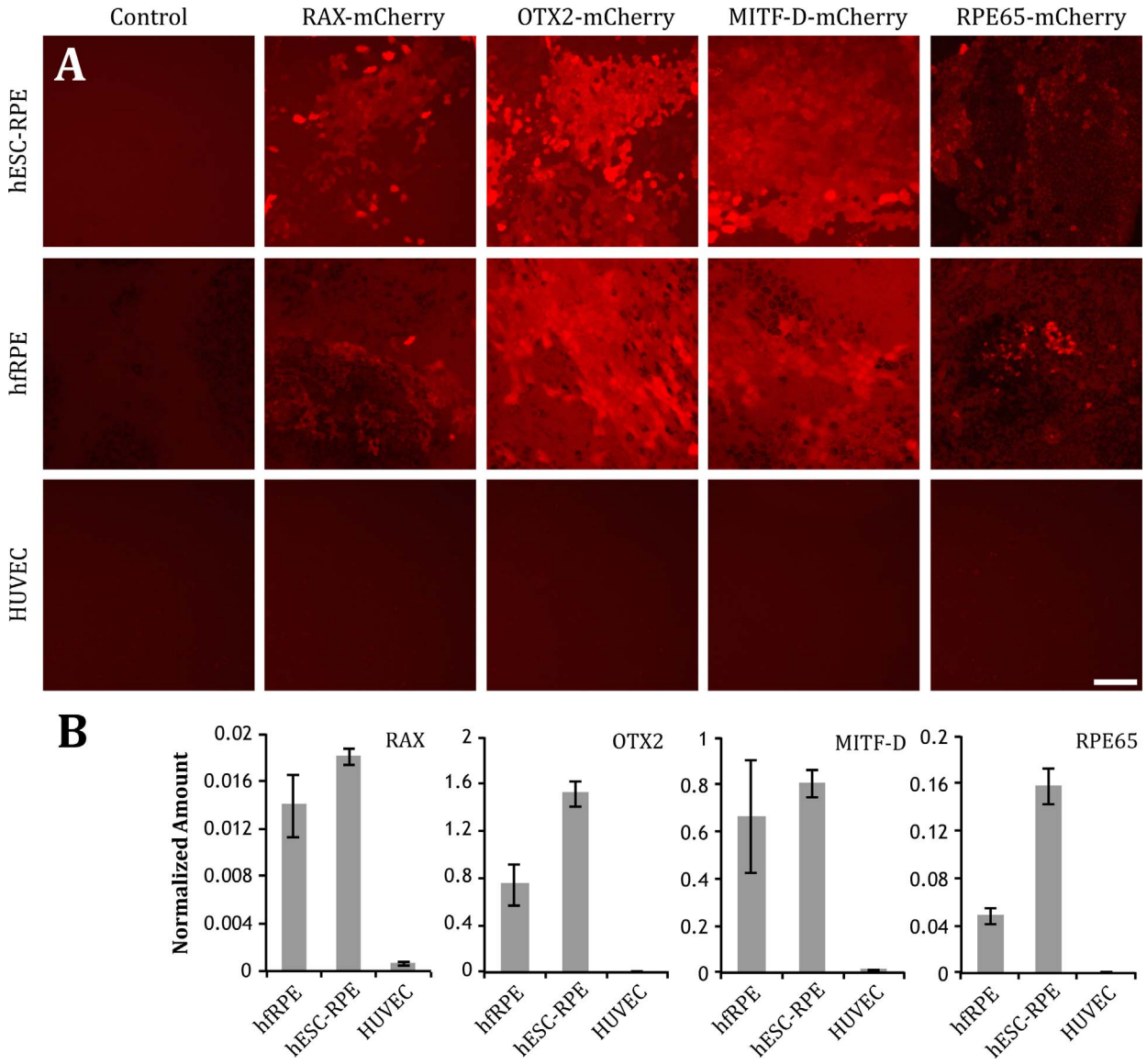

Figure 1. Fluorescent reporters are RPE-specific and reflect endogenous gene expression. (**A**) Fluorescent images show that RAX-, OTX2-, MITF-D–, and RPE65-mCherry reporters are expressed in hESC (H9)–RPE and hfRPE, but not in negative control endothelial cells (HUVECs) after 4 weeks in culture. *Scale bar* represents 100 μm. (**B**) Quantitative real-time PCR analysis of RPE-specific endogenous gene expression correlates with reporter fluorescence. *Error bars* represent the standard error of the mean (SEM).

reporter stem cell lines labeled positive for native RPE markers (OTX2, MITF, ZO-1, PMEL17, and RPE65), similar to untransduced UCSF4-RPE (Fig. 3A). Additionally, all lines were negative for the pluripotent marker TRA1-81 (Fig. 3A). Retinal pigment epithelium derived from all stable lines secreted levels of PEDF similar to untransduced UCSF4-RPE (Fig. 3B).

Wnt Signaling Pathway Genes Are Expressed During Differentiation to RPE

Next, we examined if components of the Wnt pathway were activated during later-stage RPE differentiation, as suggested by developmental studies in model organisms. The PCR array data showed that UCSF4-derived cells differentiating from day 8 to 12 express genes typically associated with the canonical/β-catenin Wnt pathway, including *LEF1*[37,38] and *WNT3*[39] (Fig. 4). Genes indicative of noncanonical Wnt pathway activation, *DAAM1*[40] and *WNT5A*,[41] were upregulated as well (Fig. 4). Increased expression of several canonical/β-catenin Wnt pathway inhibitors—*DAB2*,[42] *CXXC4*,[43] *DKK3*, and *GSK3α*[44]—was observed (Fig. 4); however, canonical/β-catenin Wnt transcriptional targets—*BTRC*,[45] *CCND1*,[46] and *LEF1*[47]—also increased significantly as UCSF4-derived cells differentiated from day 8 to 12 (Fig. 4). From these data, we next tested whether stimulating the canonical/β-catenin Wnt signaling pathway would improve RPE derivation.

Stimulation of Canonical Wnt Signaling Pathway Improves 14-Day Differentiation Protocol

The 14-day protocol was modified to include CHIR99021 in addition to activin A and the fibroblast growth factor pathway inhibitor SU5402 from days 8 to 14[9] (Fig. 5A). When using two reporter hESC lines, differences in fluorescence between control (original 14-day method) and CHIR99021-modified conditions were observed. OTX2-mCherry-UCSF4 differentiated with CHIR99021 modification showed decreased contaminant cell projections (Fig. 5B, white arrowheads) when

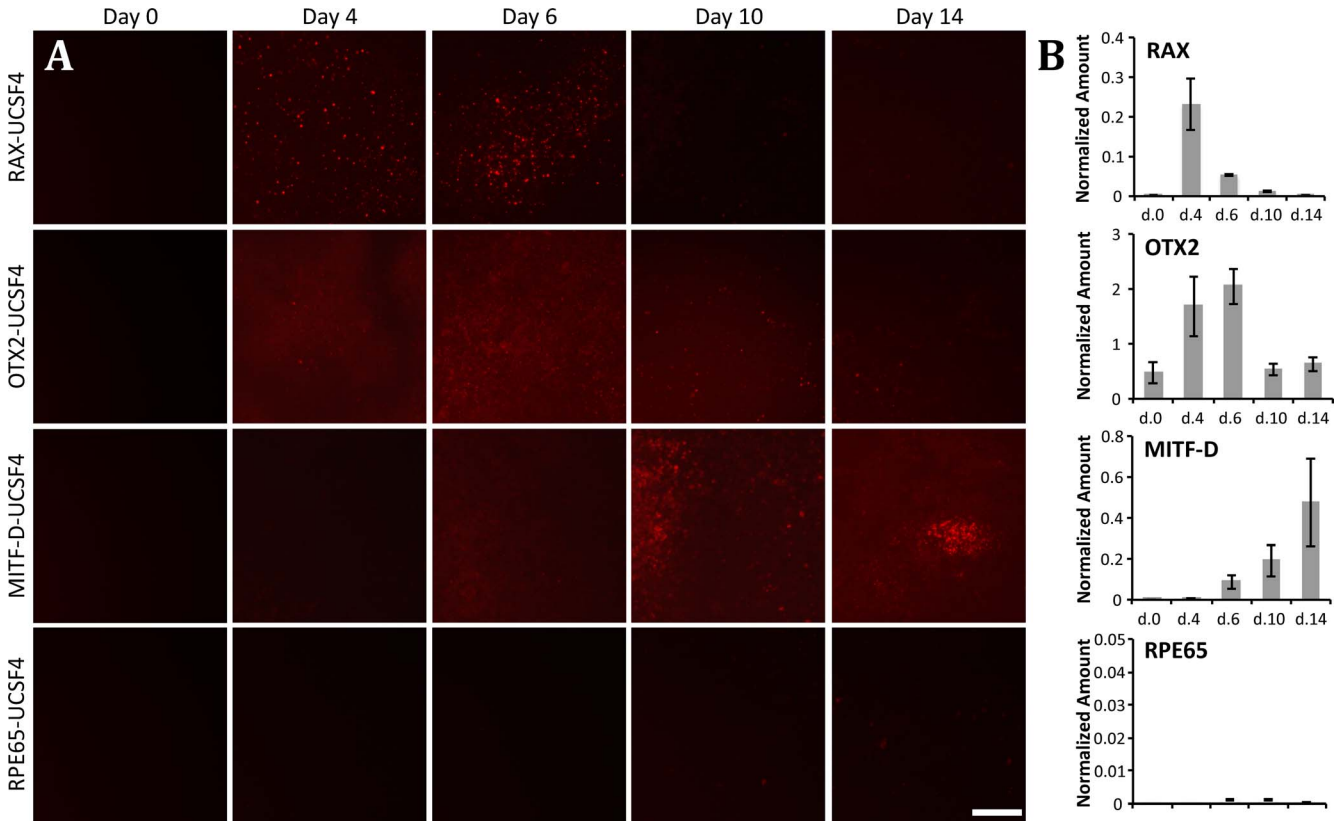

Figure 2. Fluorescent reporters reflect endogenous gene expression during directed differentiation to RPE. (**A**) Fluorescent images show RAX-, OTX2-, MITF-D–, and RPE65-mCherry reporter expression in stably transduced UCSF4 hESCs during directed differentiation. RAX- and OTX2-mCherry reporters are expressed earliest in differentiation (days 4–6). MITF-D–mCherry reporter expression was detected later in directed differentiation (days 10–14). RPE65-mCherry reporter fluorescence was not detected during differentiation. *Scale bar* is 100 μm. (**B**) Quantitative real-time PCR analysis of endogenous *RAX*, *OTX2*, *MITF-D*, and *RPE65* expression during directed differentiation is shown. *Error bars* represent ±SEM.

compared to control 14 days post differentiation (Fig. 5B). Fluid-filled domes indicating functional epithelial fluid transport[48] surrounded patches of RPE with punctate OTX2-mCherry fluorescence in CHIR99021-treated wells, but not in the control (Fig. 5B, black arrowheads). Areas absent of fluorescent signal and pigmentation were present in RPE65-mCherry-UCSF4 control wells (Fig. 5C, asterisks), indicating non-RPE cell contaminants 30 days post differentiation. The RPE derived with CHIR99021 modification, however, showed an uninterrupted monolayer of RPE65-mCherry fluorescing cells, and higher magnification images showed that cells were also more pigmented than control RPE (Fig. 5C).

Because GSK3β is centrally involved in several regulatory pathways,[49] 3 μM CHIR99021 was replaced with 100 ng/mL WNT3A or 100 ng/mL WNT5A in differentiating UCSF4 from days 8 to 14 to compare known modulators of canonical/β-catenin[39] and noncanonical[41] Wnt signaling, respectively. Immunocytochemistry performed on day 14 showed positive labeling for MITF and the neural retina–specific transcription factor CHX10 when cells were differentiated in control day 8 to 14 media (activin A + SU5402) or when media was supplemented with WNT5A (Fig. 6A). In contrast, almost no CHX10 expression was observed on day 14 in cultures differentiated with CHIR99021 or WNT3A; instead, labeled cells were positive for MITF (Fig. 6A).

The qRT-PCR analysis supported these data and showed *MITF* expression increased significantly when WNT3A or CHIR99021 was added to differentiating cultures, as compared to control or WNT5A (Fig. 6B). In addition, levels of *OTX2* expression were measured, as β-catenin has been reported to bind and activate both Mitf and Otx2 promoter elements.[18] Like *MITF, OTX2* expression was significantly upregulated in WNT3A- or CHIR99021-treated cultures, compared to control samples (Fig. 6C). Adding WNT5A resulted in increased *OTX2* expression from control, and differences did not vary significantly from WNT3A- or CHIR99021-induced expression levels (Fig. 6C). Consistent with the ICC findings, WNT3A or CHIR99021 treatment led to significant decreases in detectable *CHX10* transcript levels (Fig. 6D). WNT5A decreased *CHX10* expression somewhat, but WNT3A- or CHIR99021-treated cultures showed significantly lower CHX10 expression (Fig. 6D). These data indicate that both CHIR99021 and WNT3A decreased neural transcription factor expression and increased RPE lineage-specific transcription factor expression.

To quantify RPE derivation efficiency, cells were fixed on day 14 and analyzed for positive PMEL17 expression by flow cytometry. Derivation efficiency using the control 14-day differentiation method was 84.85%, based on PMEL17 positive cells (±5.9%, $n = 3$; Fig. 7A), which is consistent with previous findings.[9] However, CHIR99021-differentiatied UCSF4 yielded significantly more PMEL17 positive cells at day 14 (97.77% ± 0.1%, $n = 3$; Fig. 7A).

Next, cultures were grown for an additional 2 weeks in X-VIVO 10 post differentiation without enrichment to allow pigment granules to mature. Control culture wells showed minimal pigmentation (Fig. 7B) and contained non-RPE contaminating cell types that extended neural tracks throughout the culture well (Fig. 7C, arrowheads). In contrast, cultures

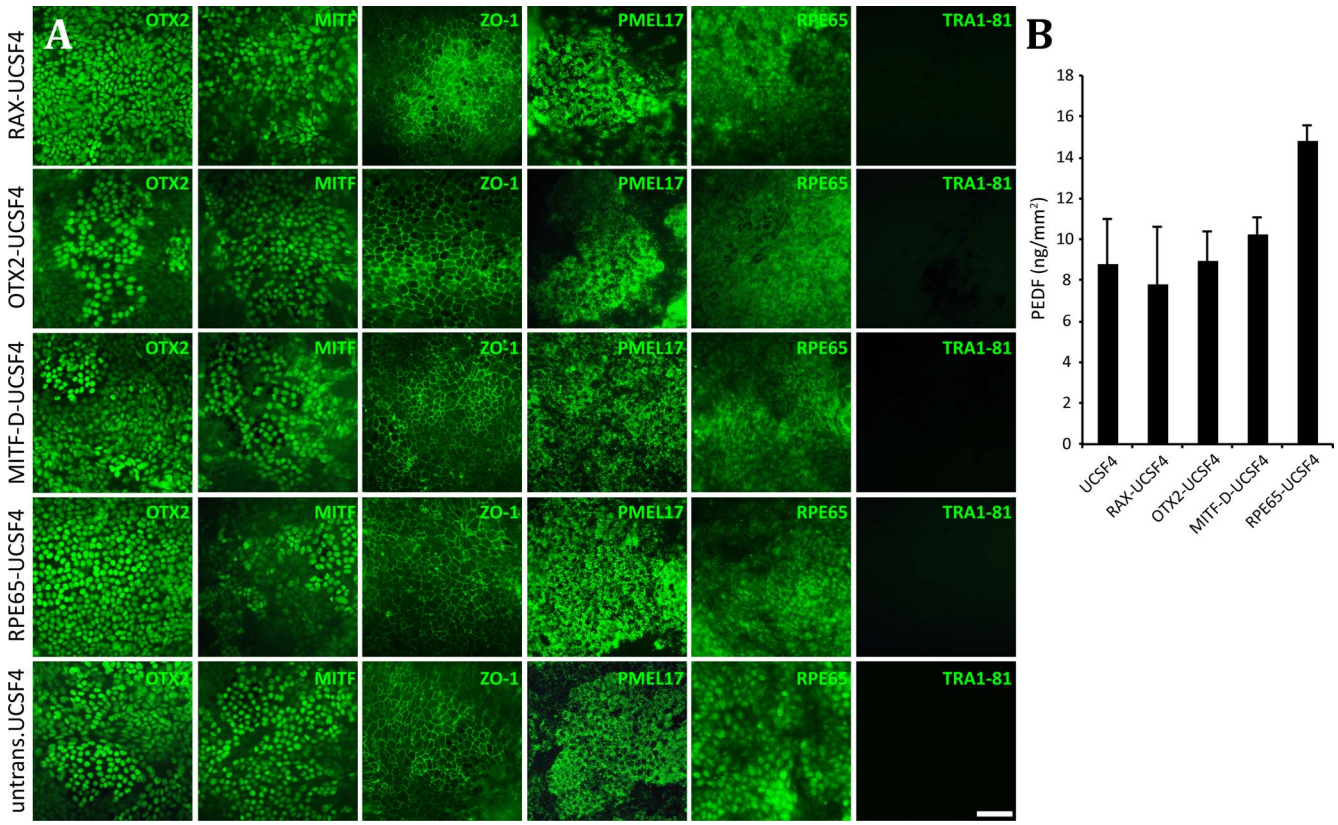

Figure 3. Viral integration does not affect RPE differentiation from stably transduced UCSF4. (**A**) Immunofluorescence images of OTX2, MITF, ZO-1, PMEL17, RPE65, and TRA1-81 are shown for UCSF4-RPE (passage 0) derived from all reporter stem cell lines and untransduced UCSF4-RPE. *Scale bar* represents 50 μm. (**B**) Secretion levels of PEDF are shown for untransduced UCSF4-RPE and all reporter UCSF4-RPE (72-hour media incubation, all lines are passage 0). *Error bars* represent ±SEM.

differentiated with CHIR99021 showed a monolayer of darkly pigmented cells (Fig. 7D) and improved cuboidal RPE morphology (Fig. 7E, inset). Fluid-filled domes also appeared in these wells (Fig. 7E, dotted line). In addition, differences in melanogenesis markers (TYR, TYRP2, and PMEL17) and the functional marker PEDF were quantified by qRT-PCR. Expression levels of *TYRP2*, *PMEL17*, and *PEDF* increased significantly in cultures differentiated with CHIR99021 (Fig. 7F). *TYR* expression levels, although increased in CHIR99021-treated cultures, were not statistically significant (Fig. 7F).

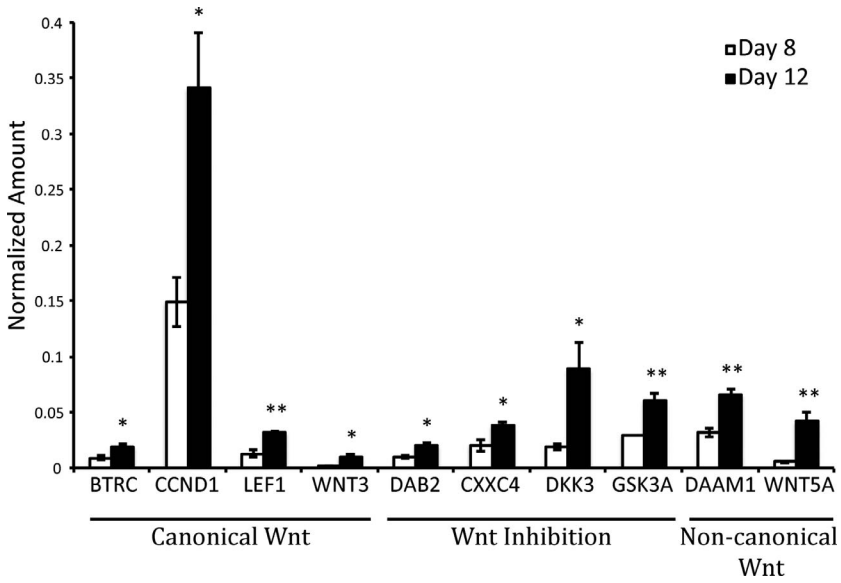

Figure 4. Components of Wnt signaling are expressed during directed differentiation of UCSF4 to RPE. Wnt array expression data showing genes upregulated from day 8 (*white*) to day 12 (*black*) of unmodified 14-day directed differentiation. *Error bars* represent ±SEM. $^{*}P \leq 0.05$, $^{**}P \leq 0.01$.

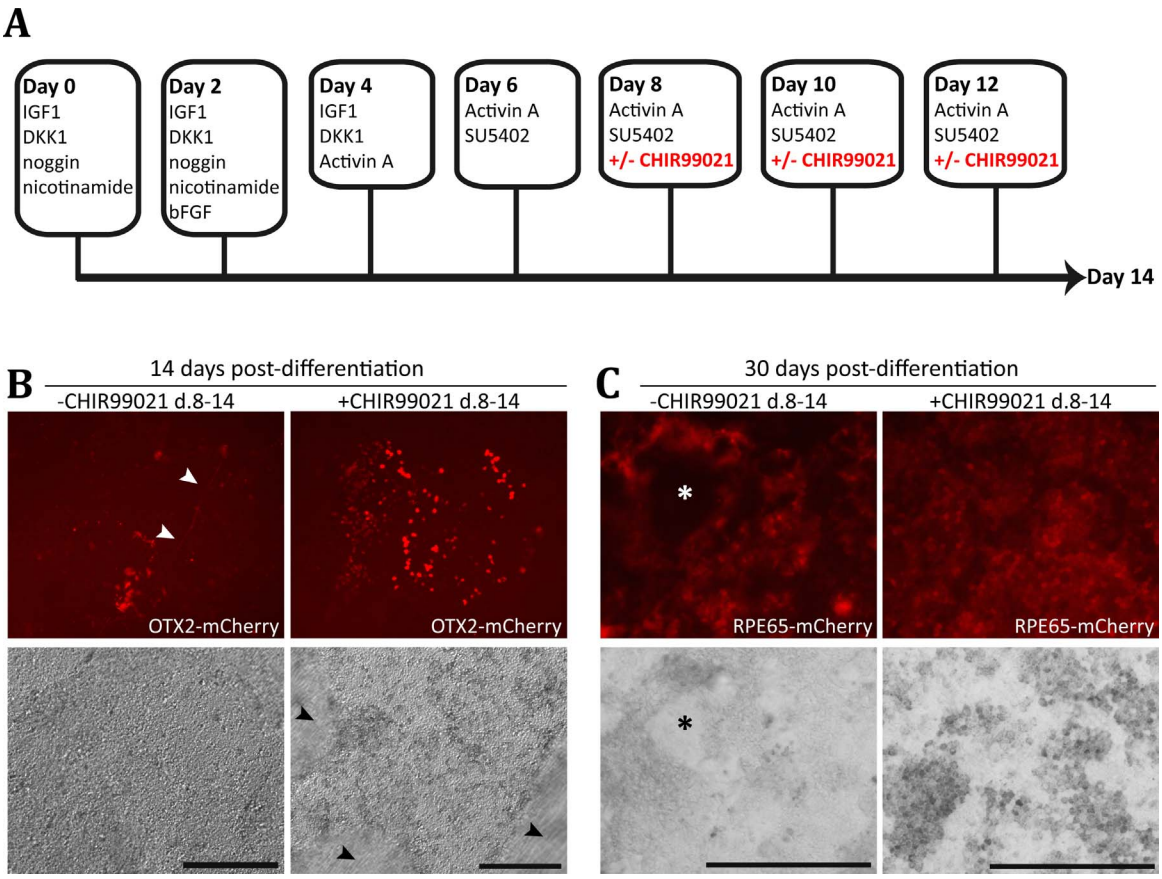

Figure 5. Addition of Wnt agonist, CHIR99021, to 14-day differentiation protocol increases fluorescent reporter expression. (**A**) Changes in media composition during 14 days of differentiation. Media components in *black* have been previously described as important for directing pluripotent cells to RPE,[9] CHIR99021 (*red*) was added from day 8 to 14 in this system. Figure adapted from Buchholz et al.[9] (**B**) Fluorescent and relief phase contrast images of OTX2-mCherry-UCSF4 RPE 14 days post differentiation by control 14-day protocol (*left panel*) or CHIR99021-modified 14-day protocol (*right panel*). *White arrowheads* indicate OTX2-positive cell projection. *Black arrowheads* designate areas where domes are present. (**C**) Fluorescent and bright field images of RPE65-mCherry-UCSF4 RPE 30 days post differentiation by control 14-day protocol (*left panel*) or CHIR99021-modified 14-day protocol (*right panel*). *Asterisks* indicate RPE65-mCherry–negative cell contaminants. (**B**, **C**) *Scale bars* represent 100 μm.

CHIR99021-Derived UCSF4-RPE Cells Are Functional After Passaging and Cryopreservation

HESC-RPE cells can be expanded for several passages and cryopreserved to create an ICB.[31] Therefore, the functionality of differentiated cells after enrichment, expansion to passage 2, cryopreservation at passage 2, and subsequent thawing to passage 3 was tested. Fluorescent images (ICC) of thawed passage-3 UCSF4-RPE cells derived with CHIR99021 addition showed expression of the RPE-specific protein markers OTX2, MITF, PMEL17, RPE65, and ZO-1 with expected localization (Fig. 8A). Cells also stained negative for TRA1-81 (Fig. 8A). Interestingly, control 14-day–derived RPE stained positive for CHX10 even after expansion to passage 3, whereas RPE cells derived with CHIR99021 were negative for CHX10 (Fig. 8B).

The ability to carry out phagocytosis of ROS is a physiologically important RPE function that can be measured in vitro by using fluorescently labeled bovine ROS.[33] Compared with HUVECs (negative control), passage-3 CHIR99021-derived UCSF4-RPE cells internalized significantly more ROS (Fig. 8C). In fact, these RPE cells outperformed the hfRPE control in this experiment. Rod outer segment internalization was blocked with an antibody against integrin αVβ5, indicating UCSF4-RPE cells bind ROS for phagocytosis by using the same receptor as hfRPE.[33] Results from a PEDF ELISA showed a significant increase in apical PEDF secretion compared to basal PEDF secretion when passage-3 CHIR99021-derived UCSF4-RPE cells were grown on transwell inserts (Fig. 8D). Results from a VEGF ELISA showed a slight increase in levels of basal VEGF secretion, compared to apical secretion, in passage-3 CHIR99021-derived UCSF4-RPE cells grown on transwell inserts; however, this difference was not significant (Fig. 8D). Polarized secretion levels of PEDF and VEGF for passage-3 CHIR99021-derived UCSF4-RPE cells were similar to those of passage-1 hfRPE cells, with no significant differences found between the two lines (Fig. 8D). Additionally, CHIR99021-derived UCSF4-RPE cells were found to lose typical RPE morphology after passage 5, when using an extended passage protocol[32] (Supplementary Fig. S1), which is consistent with previous findings of cultured RPE cells.[32,50,51] Passaging of RPE beyond passage 5 results in acquisition of a more fibroblast-like morphology and has been shown to correlate with loss of RPE function.[52]

Discussion

As AMD therapies get closer to the clinic, it will be important to develop methods that generate the highest-quality RPE for use in humans; uncovering the biological mechanisms of human RPE development from cultured hESCs is an integral part of that process. Previous reports have made use of lineage-specific fluorescent reporters when developing protocols to direct differentiation.[27,53] The results presented here describe

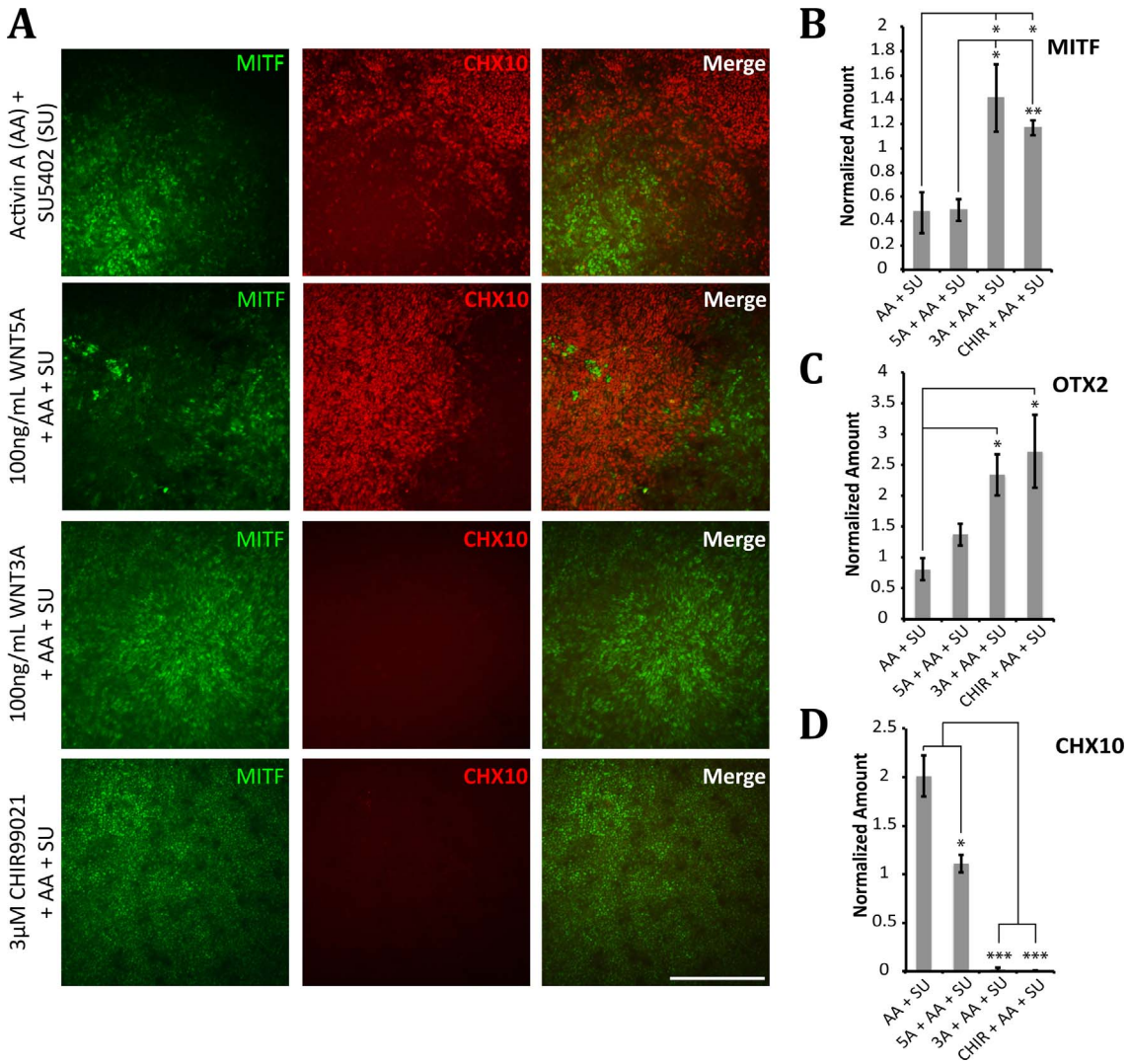

Figure 6. Canonical/β-catenin Wnt signaling influences RPE- and neural retina–specific transcription factor expression. (**A**) Immunofluorescence images show staining for RPE (MITF) and neural retinal contaminant (CHX10) proteins in UCSF4 cultures differentiated with control media (100 ng/mL activin A + 10 μM SU5402) supplemented with 100 ng/mL WNT5A, 100 ng/mL WNT3A, or 3 μM CHIR99021 at day 14. *Scale bar* represents 100 μm. (**B**) Quantitative real-time PCR of *MITF* gene expression. (**C**) Quantitative real-time PCR of *OTX2* gene expression. (**D**) Quantitative real-time PCR of *CHX10* gene expression. **(B–D)** *Error bars* represent ±SEM. $^{*}P \leq 0.05$, $^{**}P \leq 0.01$, $^{***}P \leq 0.001$.

a set of fluorescent reporters that mirror endogenous gene expression during directed differentiation to RPE. Further, we showed that activating canonical/β-catenin Wnt signaling with CHIR99021 improved RPE derivation efficiency from human pluripotent cells. CHIR99021-derived RPE were also more pigmented, exhibited better morphology without enrichment, and were functional after expansion with intermediate cryopreservation.

RAX and OTX2 are expressed early in eye field development,[54] while MITF is expressed during optic vesicle formation.[36] MITF, OTX2, and RPE65 expression is maintained in mature RPE. Together, these are ideal markers for visualizing cells differentiating from pluripotency, to the early eye field, to RPE. Of the four reporter lines generated, we found RAX- and RPE65-mCherry hESCs were the most robust, which could be due to inherent promoter strength or to silencing of OTX2- and MITF-D–mCherry transgenes post transduction. Silencing of internal promoters in SIN lentiviral vectors has been previously observed in stem cells.[55] Chromosomal positioning or the number of integrated transgene copies is another possible explanation; however, OTX2- and MITF-D–mCherry hESC lines were generated several times with little visible difference in reporter efficiency.

Previous analysis of *RAX* and *MITF* expression correlates with the reporter activity we showed in this study.[9] OTX2 reporter activation corresponds with first addition of the RPE-promoting signal, activin A, to the differentiation media. This is consistent with the role OTX2 has as a transcriptional regulator of RPE lineage, and OTX2 reporter fluorescence was also observed 14 days after differentiation when cells are more mature. However, there was a lull in reporter fluorescence on differentiation days 10 and 14, which might indicate transient OTX2 suppression during RPE differentiation. This could be isoform-specific (the *OTX2* isoform A promoter region was used); alternatively, it could be an artifact of our culture conditions or the hESC line itself. While RPE65 reporter fluorescence was not observed during the first 14 days of differentiation, fluorescence was detected in RPE 30 days post differentiation, consistent with RPE65 expression in mature RPE.

Recent studies have shown that canonical/β-catenin Wnt pathway agonists improve RPE differentiation in 3D optic-cup

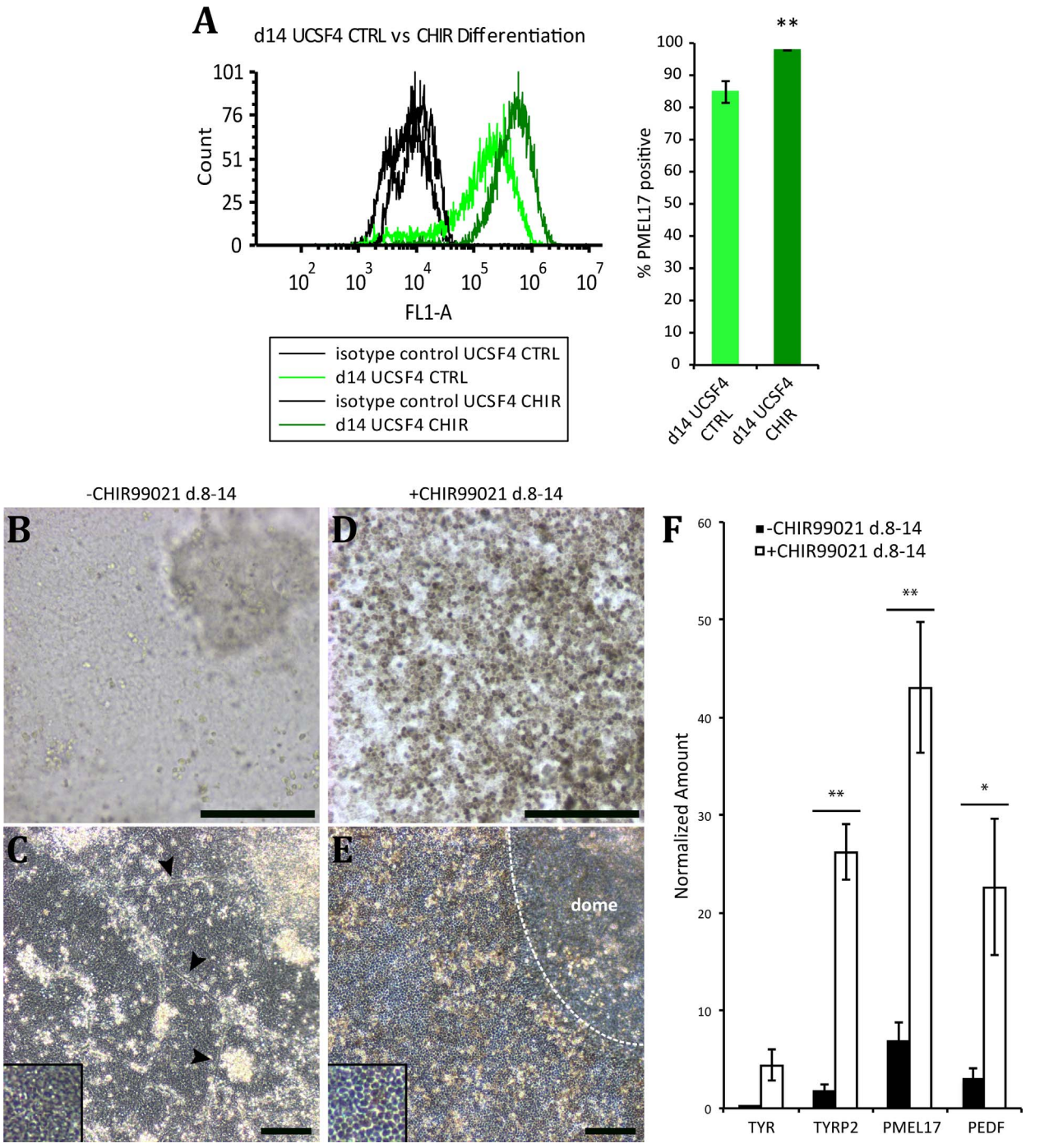

Figure 7. CHIR99021 improves RPE derivation and pigmentation. (**A**) Representative *histograms* and quantification of PMEL17 detection by flow cytometry after 14 days of differentiation, using the original protocol (d14 UCSF4 CTRL) or with 3 μM CHIR99021 modification (d14 UCSF4 CHIR). Bright field (**B**, **D**) and phase contrast (**C**, **E**) images show cells 14 days post 14-day differentiation, derived without (**B**, **C**) or with (**D**, **E**) 3 μM CHIR99021 from day 8 to 14. (**C**) *Arrowheads* indicate neural tracks. (**E**) *Dotted line* indicates edge of dome. (**C**, **E**) *Insets* show RPE morphology. *Scale bars* represent 100 μm. (**F**) Quantitative real-time PCR analysis of pigment (*TYR*, *TYRP2*, and *PMEL17*) and RPE function (*PEDF*) gene expression in cultures 14 days post 14-day differentiation, derived with or without CHIR99021. (**A**, **F**) *Error bars* represent ±SEM. $^{*}P \leq 0.05$, $^{**}P \leq 0.01$.

structures forming from mouse ESCs,[53] and CHIR99021 increases MITF expression and pigmentation in a similar culture system differentiating from hESCs.[20] Consistent with these findings, we reported that adding CHIR99021 or WNT3A for 6 days (day 8–14) increased MITF expression levels in differentiating RPE. Likewise, RPE allowed to mature after CHIR99021-modified differentiation showed improvements in pigmentation and expression of melanogenesis markers. We also detected upregulation of *OTX2*, which is consistent with the finding that β-catenin can bind and regulate *Otx2* and *Mitf* promoters.[13,17] Previous developmental studies have shown that Chx10 represses Mitf, promoting neural retina identity over RPE.[36,56,57] Importantly, we showed decreased CHX10-positive neural retina contaminants at both the protein and

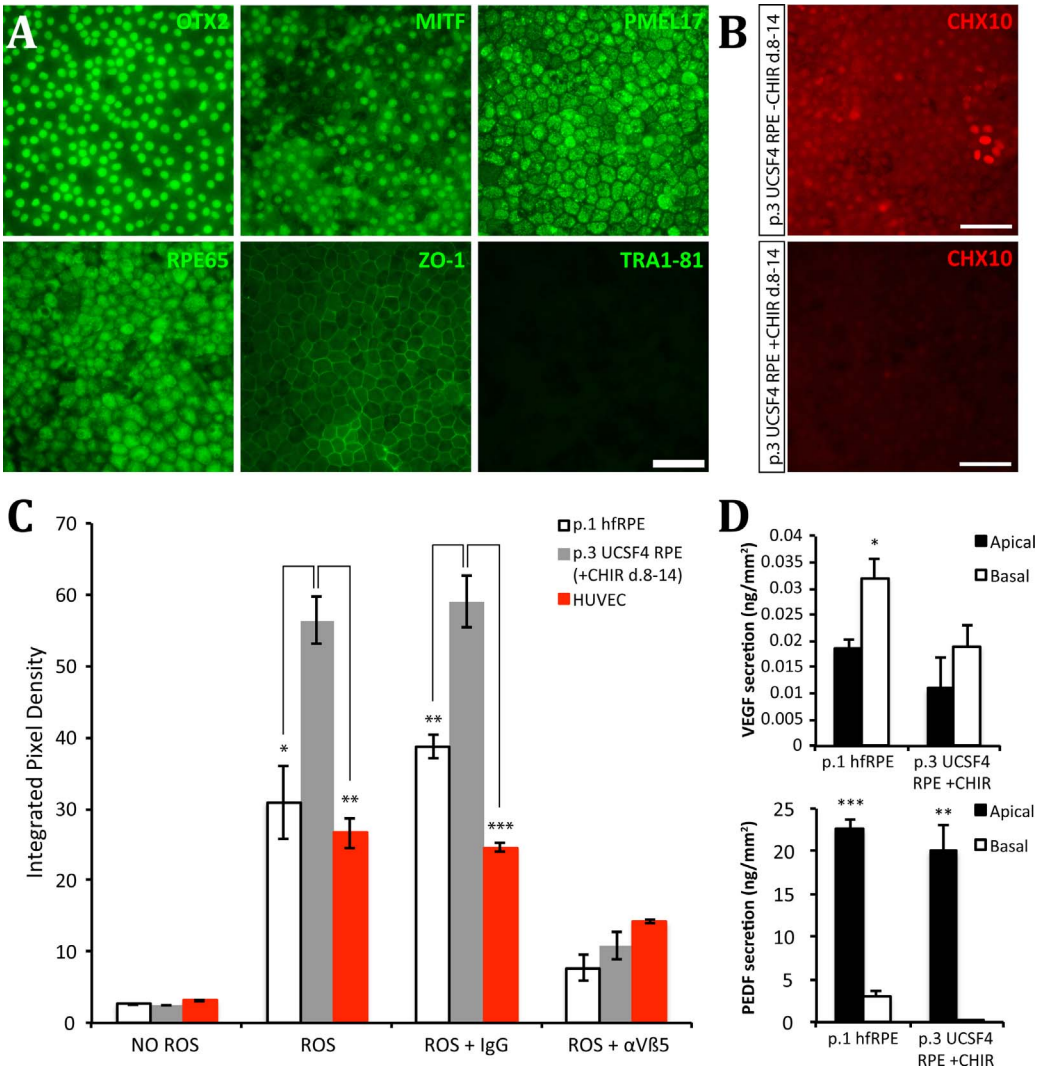

Figure 8. Analysis of day-30 UCSF4-RPE post thaw to passage 3 (p.3). (**A**) Day-30 UCSF4 p.3 RPE + CHIR day 8 to 14 (d.8–14) immunofluorescence images of OTX2, MITF, PMEL17, RPE65, ZO-1, and TRA1-81 are shown. (**B**) Immunofluorescence images of CHX10 for UCSF4 p.3 RPE with and without CHIR99021 during d.8–14 of differentiation are shown. (**A**, **B**) *Scale bars* represent 50 μm. (**C**) Levels of bovine ROS internalization measured by pixel density of fluorescence micrographs are shown for UCSF4 p.3 RPE + CHIR d.8–14 and compared to hfRPE and negative control endothelial cells (HUVECs). (**D**) Apical and basal secretion levels of PEDF and VEGF from day-30 UCSF4 p.3 RPE + CHIR d.8–14 are shown, compared to day-30 p.1 hfRPE (24-hour media incubation). (**C**, **D**) *Error bars* represent ±SEM. $^{*}P \leq 0.05$, $^{**}P \leq 0.01$, $^{***}P \leq 0.001$.

transcript level when cells were differentiated with CHIR99021 or WNT3A. This indicates that Wnt signaling aids in suppressing CHX10 expression as hESCs differentiate to RPE, perhaps directly or indirectly through *MITF* and *OTX2* activation.

Activin A promotes RPE differentiation by upregulating *Mitf* and subsequently downregulating *Chx10* during development,[58] and other differentiation studies, including our own, have used activin A to direct ESC to RPE.[9–11] However, even in our own efforts, we report incomplete conversion (~80% RPE derivation efficiency). Interestingly, we found that CHX10 expression persists in culture wells derived with activin A and SU5402 after expansion and multiple rounds of passaging. These findings, together with the reported effects of CHIR99021 and WNT3A on CHX10, indicate Wnt signaling could work synergistically with activin A to fully promote an RPE lineage from hESCs, and cooperation of these signaling pathways has been previously described.[59,60]

Developing the original 14-day differentiation method has revealed that the degree and timing of initial pigmentation inversely correlates with RPE derivation efficiency, indicating signals from neighboring, non-RPE cells might influence differentiation in vitro.[9] The Wnt array identified overexpression of two ligands as cells progressed to RPE: WNT3 and WNT5A. We found that WNT3A (highly similar to WNT3[61]), but not WNT5A, was able to recapitulate the effects of CHIR99021, indicating WNT3 could be an RPE-promoting ligand in differentiating hESCs. Notably, both *Wnt3* and *Wnt5a* are expressed in the developing murine neural retina[15] and in chick RPE, with *Wnt5a* expression appearing in the surrounding mesenchyme and neural retina earlier in chick eye development.[62] Further examining which cells express these specific ligands during RPE differentiation could provide insight into what tissues produce lineage-promoting signals in human eye development.

Improving RPE derivation is an important step in translating cellular therapies. Methods currently used for AMD clinical trials[31] report efficient RPE derivation; however, it takes many weeks before pigmented foci are large enough to be manually enriched and expanded. We reported that, on average, 97.77%

of cells differentiated when using our CHIR99021-modified method are PMEL17 positive by day 14, which is approximately 2 weeks faster than directed differentiation protocols reporting similar efficiency.[10] Such high efficiency derivation requires little manipulation and enrichment on day 14, which is ideal for translating methods for clinical use, as passaging RPE can result in epithelial to mesenchymal transition.[50] We demonstrated that CHIR99021-derived hESC-RPE cells have typical morphology, domes, and pigmentation at day 28 without enrichment. Thus, it is plausible these RPE cells will not require several rounds of in vitro passaging to eliminate non-RPE cell contaminants and will be suitable for clinical use. Further work will be required to convert this protocol to be compatible with good manufacturing practices.

We showed that after the CHIR99021-modified protocol, cells obtained can be further passaged for three passages (but not beyond five passages). After three passages, cells form polarized monolayers and express RPE markers, and functions. They show apical secretion of PEDF and basal secretion of VEGF.

Taken together, these findings validate a set of molecular tools with an application potential much wider than the scope of this study. Additionally, we highlight how hESC-directed differentiation models can be used to better understand human RPE development, which has important implications for translating cell-based AMD therapies to the clinic.

Acknowledgments

We thank Sherry Hikita, PhD, Michelle Maloney, Cassidy Hinman, and staff of the Laboratory for Stem Cell Biology and Engineering (University of California, Santa Barbara [UCSB]) for providing pluripotent stem cells and advice on stem cell and RPE maintenance and culturing, and also Mary Raven, PhD, director of the Neuroscience Research Institute/Molecular, Cellular & Developmental Biology (NRI/MCDB) Microscopy Facility (UCSB), for her expertise in fluorescence microscopy.

Supported by the Garland Initiative for Vision, the California Institute for Regenerative Medicine (CIRM; Grants DR1-01444, CL1-00521, TB1-01177, TG2-01151 [DOC]), Fight for Sight, the Foundation Fighting Blindness Wynn-Gund Translational Research Acceleration Program, the University of California Santa Barbara Institute for Collaborative Biotechnologies from the U.S. Army Research Office (Grant W911NF-09-0001), and CIRM Major Facilities Grant (FA1-00616). LLL was a fellow of the Vermont Community Foundation. VPN was a fellow of the CIRM Bridges program. The content within does not necessarily reflect the position or policy of the government, and endorsement should not be inferred.

Disclosure: **L.L. Leach**, None; **D.E. Buchholz**, None; **V.P. Nadar**, None; **S.E. Lowenstein**, None; **D.O. Clegg**, Regenerative Patch Technologies (C)

References

1. Friedman DS, O'Colmain BJ, Muñoz B, et al. Prevalence of age-related macular degeneration in the United States. *Arch Ophthalmol*. 2004;122:564–572.
2. Klein R, Chou C-F, Klein BEK, Zhang X, Meuer SM, Saaddine JB. Prevalence of age-related macular degeneration in the US population. *Arch Ophthalmol*. 2011;129:75–80.
3. Klaver CC, Wolfs RC, Vingerling JR, Hofman A, De Jong PT. Age-specific prevalence and causes of blindness and visual impairment in an older population: the Rotterdam Study. *Arch Ophthalmol*. 1998;116:653–658.
4. Clegg DO, Hikita ST, Hu Q, et al. Derivation of retinal pigmented epithelial cells for the treatment of ocular disease. In: *Stem Cells Handbook*. 2nd Ed. New York, NY: Springer Publishing; 2013:411–418.
5. Rowland TJ, Buchholz DE, Clegg DO. Pluripotent human stem cells for the treatment of retinal disease. *J Cell Physiol*. 2011; 227:457–466.
6. Buchholz DE, Hikita ST, Rowland TJ, et al. Derivation of functional retinal pigmented epithelium from induced pluripotent stem cells. *Stem Cells*. 2009;27:2427–2434.
7. Vugler A, Carr A-J, Lawrence J, et al. Elucidating the phenomenon of HESC-derived RPE: anatomy of cell genesis, expansion and retinal transplantation. *Exp Neurol*. 2008;214: 347–361.
8. Klimanskaya I, Hipp J, Rezai KA, West M, Atala A, Lanza R. Derivation and comparative assessment of retinal pigment epithelium from human embryonic stem cells using transcriptomics. *Cloning Stem Cells*. 2004;6:217–245.
9. Buchholz DE, Pennington BO, Croze RH, Hinman CR, Coffey PJ, Clegg DO. Rapid and efficient directed differentiation of human pluripotent stem cells into retinal pigmented epithelium. *Stem Cells Transl Med*. 2013;2:384–393.
10. Zhu Y, Carido M, Meinhardt A, et al. Three-dimensional neuroepithelial culture from human embryonic stem cells and its use for quantitative conversion to retinal pigment epithelium. *PLoS ONE*. 2013;8:e54552.
11. Idelson M, Alper R, Obolensky A, et al. Directed differentiation of human embryonic stem cells into functional retinal pigment epithelium cells. *Stem Cell*. 2009;5:396–408.
12. Osakada F, Jin Z-B, Hirami Y, et al. In vitro differentiation of retinal cells from human pluripotent stem cells by small-molecule induction. *J Cell Sci*. 2009;122(pt 17):3169–3179.
13. Westenskow P, Piccolo S, Fuhrmann S. Beta-catenin controls differentiation of the retinal pigment epithelium in the mouse optic cup by regulating Mitf and Otx2 expression. *Development*. 2009;136:2505–2510.
14. Steinfeld J, Steinfeld I, Coronato N, et al. RPE specification in the chick is mediated by surface ectoderm-derived BMP and Wnt signalling. *Development*. 2013;140:1–11.
15. Liu H, Mohamed O, Dufort D, Wallace VA. Characterization of Wnt signaling components and activation of the Wnt canonical pathway in the murine retina. *Dev Dyn*. 2003;227: 323–334.
16. Zakin LD, Mazan S, Maury M, Martin N, Guénet JL, Brûlet P. Structure and expression of Wnt13, a novel mouse Wnt2 related gene. *Mech Dev*. 1998;73:107–116.
17. Fujimura N, Taketo MM, Mori M, Korinek V, Kozmik Z. Spatial and temporal regulation of Wnt/β-catenin signaling is essential for development of the retinal pigment epithelium. *Dev Biol*. 2009;334:31–45.
18. Westenskow PD, McKean JB, Kubo F, Nakagawa S, Fuhrmann S. Ectopic Mitf in the Embryonic Chick Retina by Co-transfection of -Catenin and Otx2. *Invest Ophthalmol Vis Sci*. 2010;51:5328–5335.
19. Lamba DA, McUsic A, Hirata RK, Wang P-R, Russell D, Reh TA. Generation, purification and transplantation of photoreceptors derived from human induced pluripotent stem cells. *PLoS ONE*. 2010;5:e8763.
20. Nakano T, Ando S, Takata N, et al. Self-formation of optic cups and storable stratified neural retina from human ESCs. *Cell Stem Cell*. 2012;10:771–785.
21. Fuhrmann S. Wnt signaling in eye organogenesis. *Organogenesis*. 2008;4:60–67.
22. Diniz B, Thomas P, Thomas B, et al. Subretinal implantation of retinal pigment epithelial cells derived from human embryonic stem cells: improved survival when implanted as a monolayer. *Invest Ophthalmol Vis Sci*. 2013;54:5087–5096.
23. Maminishkis A, Chen S, Jalickee S, et al. Confluent monolayers of cultured human fetal retinal pigment epithelium exhibit morphology and physiology of native tissue. *Invest Ophthalmol Vis Sci*. 2006;47:3612–3624.

24. Courtois V, Chatelain G, Han Z-Y, Le Novère N, Brun G, Lamonerie T. New Otx2 mRNA isoforms expressed in the mouse brain. *J Neurochem*. 2003;84:840–853.
25. Takeda K, Yasumoto KI, Kawaguchi N, et al. Mitf-D, a newly identified isoform, expressed in the retinal pigment epithelium and monocyte-lineage cells affected by Mitf mutations. *Biochim Biophys Acta*. 2002;1574:15–23.
26. Nicoletti A, Kawase K, Thompson DA. Promoter analysis of RPE65, the gene encoding a 61-kDa retinal pigment epithelium-specific protein. *Invest Ophthalmol Vis Sci*. 2005;39:637–644.
27. Kita-Matsuo H, Barcova M, Prigozhina N, et al. Lentiviral vectors and protocols for creation of stable hESC lines for fluorescent tracking and drug resistance selection of cardiomyocytes. *PLoS ONE*. 2009;4:e5046.
28. Dull T, Zufferey R, Kelly M, et al. A third-generation lentivirus vector with a conditional packaging system. *J Virol*. 1998;72:8463–8471.
29. Beers J, Gulbranson DR, George N, et al. Passaging and colony expansion of human pluripotent stem cells by enzyme-free dissociation in chemically defined culture conditions. *Nat Protoc*. 2012;7:2029–2040.
30. Willert K, Brown JD, Danenberg E, et al. Wnt proteins are lipid-modified and can act as stem cell growth factors. *Nature*. 2003;423:448–452.
31. Schwartz SD, Hubschman J-P, Heilwell G, et al. Embryonic stem cell trials for macular degeneration: a preliminary report. *Lancet*. 2012;379:713–720.
32. Croze RH, Buchholz DE, Radeke MJ, et al. ROCK inhibition extends passage of pluripotent stem cell-derived retinal pigmented epithelium. *Stem Cells Transl Med*. 2014;3:1066–1078.
33. Lin H, Clegg DO. Integrin alphavbeta5 participates in the binding of photoreceptor rod outer segments during phagocytosis by cultured human retinal pigment epithelium. *Invest Ophthalmol Vis Sci*. 1998;39:1703–1712.
34. Martnez-Morales JR, Rodrigo I, Bovolenta P. Eye development: a view from the retina pigmented epithelium. *Bioessays*. 2004;26:766–777.
35. Meyer JS, Shearer RL, Capowski EE, et al. Modeling early retinal development with human embryonic and induced pluripotent stem cells. *Proc Natl Acad Sci U S A*. 2009;106:16698–16703.
36. Bharti K, Liu W, Csermely T, Bertuzzi S, Arnheiter H. Alternative promoter use in eye development: the complex role and regulation of the transcription factor MITF. *Development*. 2008;135:1169–1178.
37. Behrens J, Kries von JP, Kühl M, et al. Functional interaction of beta-catenin with the transcription factor LEF-1. *Nature*. 1996;382:638–642.
38. Huber O, Korn R, McLaughlin J, Ohsugi M, Herrmann BG, Kemler R. Nuclear localization of beta-catenin by interaction with transcription factor LEF-1. *Mech Dev*. 1996;59:3–10.
39. Shimizu H, Julius MA, Giarré M, Zheng Z, Brown AM, Kitajewski J. Transformation by Wnt family proteins correlates with regulation of beta-catenin. *Cell Growth Differ*. 1997;8:1349–1358.
40. Habas R, Kato Y, He X. Wnt/Frizzled activation of Rho regulates vertebrate gastrulation and requires a novel Formin homology protein Daam1. *Cell*. 2001;107:843–854.
41. Kühl M, Sheldahl LC, Park M, Miller JR, Moon RT. The Wnt/Ca2+ pathway: a new vertebrate Wnt signaling pathway takes shape. *Trends Genet*. 2000;16:279–283.
42. Hocevar BA, Mou F, Rennolds JL, Morris SM, Cooper JA, Howe PH. Regulation of the Wnt signaling pathway by disabled-2 (Dab2). *EMBO J*. 2003;22:3084–3094.
43. Hino SI, Kishida S, Michiue T, et al. Inhibition of the Wnt Signaling Pathway by Idax, a novel Dvl-binding protein. *Mol Cell Biol*. 2001;21:330–342.
44. Doble BW, Patel S, Wood GA, Kockeritz LK, Woodgett JR. Functional redundancy of GSK-3α and GSK-3β in Wnt/β-catenin signaling shown by using an allelic series of embryonic stem cell lines. *Dev Cell*. 2007;12:957–971.
45. Spiegelman VS, Slaga TJ, Pagano M, Minamoto T, Ronai Z, Fuchs SY. Wnt/beta-catenin signaling induces the expression and activity of betaTrCP ubiquitin ligase receptor. *Mol Cell*. 2000;5:877–882.
46. Shtutman M, Zhurinsky J, Simcha I, et al. The cyclin D1 gene is a target of the beta-catenin/LEF-1 pathway. *Proc Natl Acad Sci U S A*. 1999;96:5522–5527.
47. Filali M. Wnt-3A/beta-catenin signaling induces transcription from the LEF-1 promoter. *J Biol Chem*. 2002;277:33398–33410.
48. McKay BS, Irving PE, Skumatz CM, Burke JM. Cell-cell adhesion molecules and the development of an epithelial phenotype in cultured human retinal pigment epithelial cells. *Exp Eye Res*. 1997;65:661–671.
49. Hur E-M, Zhou F-Q. GSK3 signalling in neural development. *Nature Rev Neurosci*. 2010;11:539–551.
50. Grisanti S, Guidry C. Transdifferentiation of retinal pigment epithelial cells from epithelial to mesenchymal phenotype. *Invest Ophthalmol Vis Sci*. 1995;36:391–405.
51. Lee SC, Kwon OW, Seong GJ, Kim SH, Ahn JE, Kay ED. Epitheliomesenchymal transdifferentiation of cultured RPE cells. *Ophthalmic Res*. 2001;33:80–86.
52. Singh R, Phillips MJ, Kuai D, et al. Functional analysis of serially expanded human iPS cell-derived RPE cultures. *Invest Ophthalmol Vis Sci*. 2013;54:6767–6778.
53. Eiraku M, Takata N, Ishibashi H, et al. Self-organizing optic-cup morphogenesis in three-dimensional culture. *Nature*. 2011;472:51–56.
54. Bailey TJ, El-Hodiri H, Zhang L, Shah R, Mathers PH, Jamrich M. Regulation of vertebrate eye development by Rx genes. *Int J Dev Biol*. 2004;48:761–770.
55. He J, Yang Q, Chang LJ. Dynamic DNA methylation and histone modifications contribute to lentiviral transgene silencing in murine embryonic carcinoma cells. *J Virol*. 2005;79:13497–13508.
56. Horsford DJ. Chx10 repression of Mitf is required for the maintenance of mammalian neuroretinal identity. *Development*. 2004;132:177–187.
57. Rowan S, Chen C-MA, Young TL, Fisher DE, Cepko CL. Transdifferentiation of the retina into pigmented cells in ocular retardation mice defines a new function of the homeodomain gene Chx10. *Development*. 2004;131:5139–5152.
58. Fuhrmann S, Levine EM, Reh TA. Extraocular mesenchyme patterns the optic vesicle during early eye development in the embryonic chick. *Development*. 2000;127:4599–4609.
59. Teo AKK, Valdez IA, Dirice E, Kulkarni RN. Comparable generation of activin-induced definitive endoderm via additive Wnt or BMP signaling in absence of serum. *Stem Cell Reports*. 2014;3:5–14.
60. Watabe T, Kim S, Candia A, et al. Molecular mechanisms of Spemann's organizer formation: conserved growth factor synergy between Xenopus and mouse. *Genes Dev*. 1995;9:3038–3050.
61. Roelink H, Nusse R. Expression of two members of the Wnt family during mouse development—restricted temporal and spatial patterns in the developing neural tube. *Genes Dev*. 1991;5:381–388.
62. Jin E-J, Burrus LW, Erickson CA. The expression patterns of Wnts and their antagonists during avian eye development. *Mech Dev*. 2002;116:173–176.

Investigative Ophthalmology & Visual Science